



Published in final edited form as:

Diabetes. 2008 February ; 57(2): 470–475.

Attenuation of Counterregulatory Responses to Recurrent Hypoglycemia by Active Thalamic Inhibition:

A Mechanism for Hypoglycemia-Associated Autonomic Failure

Ana Maria Arbelaez, M.D., William J. Powers, M.D., Tom O. Videen, Ph.D., Joseph L. Price, Ph.D., and Philip E. Cryer, M.D.

From the Departments of Pediatrics (A.M.A.), Neurology and Radiology (W.J.P. and T.O.V.), Neurological Surgery (W.J.P.), Anatomy and Neurobiology (J.L.P.) and Medicine (P.E.C.), Washington University School of Medicine, St. Louis, Missouri and the Department of Neurology, University of North Carolina School of Medicine, Chapel Hill, North Carolina (W.J.P.)

Abstract

Objective—Hypoglycemia, the limiting factor in the glyceic management of diabetes, is the result of the interplay of therapeutic insulin excess and compromised glyceic defenses. The key feature of the latter is an attenuated sympathoadrenal response to hypoglycemia that typically follows an episode of recent antecedent iatrogenic hypoglycemia, a phenomenon termed hypoglycemia-associated autonomic failure (HAAF) in diabetes. We investigated the role of cerebral mechanisms in HAAF by measuring regional brain activation during recurrent hypoglycemia with attenuated counterregulatory responses and comparing it to initial hypoglycemia in healthy individuals.

Research Design and Methods—We used [¹⁵O]water and positron emission tomography to measure regional cerebral blood flow (CBF) as a marker of brain synaptic activity during hyperinsulinemic hypoglycemic clamps (55 mg/dL [3.0 mmol/L]) in the naïve condition (Day 1) and after ~24 hours of interval interprandial hypoglycemia (Day 2) in nine healthy adults.

Results—Interval hypoglycemia produced attenuated sympathoadrenal, symptomatic and other counterregulatory responses to hypoglycemia on Day 2, a model of HAAF. Synaptic activity in the dorsal midline thalamus during hypoglycemia was significantly greater on Day 2 than Day 1 (P=0.004).

Conclusion—Greater synaptic activity associated with attenuated counterregulatory responses indicates that the dorsal midline thalamus plays an active inhibitory role in reducing sympathoadrenal and symptomatic responses to hypoglycemia when previous hypoglycemia has occurred, the key feature of HAAF in diabetes.

Keywords

Hypoglycemia; Diabetes; Hypoglycemia-Associated Autonomic Failure; Positron Emission Tomography; Thalamus

Correspondence: Philip E. Cryer, M.D., Campus Box 8127, Washington University School of Medicine, 660 South Euclid Avenue, St. Louis, MO 63110, U.S.A. Phone: (314) 362-7635, Fax: (314) 362-7989, Email: pcryer@wustl.edu.

Disclosures

P.E. Cryer has served on Advisory Boards for Novo Nordisk Inc., Takeda Pharmaceuticals North America, MannKind Corp. and Merck and Co., and as a consultant for TolerRx Inc., Amgen Inc. and Marcadia Biotech, in recent years.

Introduction

Iatrogenic hypoglycemia is the limiting factor in the glycemc management of diabetes (1). It causes recurrent morbidity in most people with type 1 diabetes and many with advanced type 2 diabetes, and is sometimes fatal. Furthermore, the barrier of hypoglycemia precludes maintenance of euglycemia over a lifetime of diabetes and thus full realization of the long-term benefits of glycemc control. Finally, episodes of hypoglycemia further impair defenses against falling plasma glucose concentrations and therefore cause a vicious cycle of recurrent hypoglycemia.

Hypoglycemia in diabetes is the result of the interplay of therapeutic insulin excess and compromised physiological and behavioral defenses against falling plasma glucose concentrations (1-3). The key feature of the latter is an attenuated sympathoadrenal response to hypoglycemia that causes the clinical syndromes of hypoglycemia unawareness (which is largely the result of a reduced sympathetic neural response [4]) and defective glucose counterregulation (which is the result of a reduced adrenomedullary epinephrine response in the setting of absent decrements in insulin and absent increments in glucagon in insulin deficient diabetes - type 1 diabetes and advanced [i.e., absolutely insulin deficient] type 2 diabetes). These syndromes increase the risk of severe iatrogenic hypoglycemia ~6-fold (5) and 25-fold or more (6,7) respectively in type 1 diabetes. Because of the key pathophysiological role of the attenuated sympathoadrenal response, which is typically caused by recent antecedent hypoglycemia (1-3) but also follows exercise (8) and occurs during sleep (9), this phenomenon has been termed hypoglycemia-associated autonomic failure (HAAF) in diabetes (1-3). A similar phenomenon of reduced sympathoadrenal responses to hypoglycemia after a period of antecedent hypoglycemia can be produced in normal subjects and serves as a human model to study the mechanisms of HAAF (10).

The mechanisms of HAAF are not known (1). While the fundamental alteration could be in the afferent or efferent components of the sympathoadrenal system, it is often assumed to reside within the CNS. Potential mechanisms, most focused on the hypothalamus, have been reviewed (11,12).

Measurements of the increase from baseline in regional cerebral blood flow with [¹⁵O]water and positron emission tomography (PET) can be used to identify regions of increased brain synaptic activity and determine which brain regions are involved with different physiological activities (13). In normal human subjects, we have reported that hypoglycemia causes increased synaptic activity in a discrete network of interconnected brain regions including medial prefrontal cortex, orbito-prefrontal cortex, thalamus and periaqueductal grey. These structures are part of a system that mediates autonomic responses to various different stimuli (14). We have now investigated the role of cerebral mechanisms in HAAF by measuring regional brain synaptic activity during recurrent hypoglycemia with attenuated counterregulatory responses and comparing it to initial hypoglycemia.

Design and Methods

Subjects

Nine healthy young adults (4 women/5 men, mean [\pm SD] age 25 \pm 3 years, body mass index 23.7 \pm 2.8 kg/m²) gave their written informed consent to participate in this study which was approved by the Washington University Human Research Protection Office and conducted at the Washington University General Clinical Research Center (GCRC) and Neurology-Neurosurgery ICU PET Research Facility. All had negative medical histories and normal physical examinations, normal fasting plasma glucose concentrations, serum creatinine concentrations and hematocrits, and normal electrocardiograms. None had a personal or first

degree relative history of diabetes, psychiatric or neurological conditions. These were different subjects than in our previous study (14).

Experimental Design

Subjects were admitted to the GCRC and studied over two consecutive days after overnight fasts. On the morning of Day 1 two intravenous catheters were inserted into arm veins (for infusions) and one intravenous catheter was inserted into a dorsal hand vein with that hand kept in an $\sim 55^{\circ}\text{C}$ plexiglas box (for arterialized venous sampling). Hyperinsulinemic (regular human insulin, Novo Nordisk, Bagsværd, Denmark in a dose of $2.0 \text{ mU}\cdot\text{kg}^{-1}\cdot\text{min}^{-1}$) euglycemic (90 mg/dL [5.0 mmol/L] $\times \sim 2$ hours) and then hypoglycemic (55 mg/dL [3.0 mmol/L] $\times \sim 2$ hours) clamps - variable infusions of 20% dextrose based on plasma glucose determinations (YSI Glucose Analyzer 2, Yellow Springs Instruments, Yellow Springs, OH) every five minutes - were performed on the mornings of Day 1 and Day 2. [^{15}O]water positron emission tomography (PET) measurements of regional cerebral blood flow (see below) were performed four times at 15 minute intervals during the second hour of euglycemia and four times at 15 minute intervals during the second hour of hypoglycemia on both days. Arterialized venous samples for the analytes described below were drawn, blood pressures and heart rates were recorded and symptom scores were determined every 15 minutes, and the electrocardiogram was monitored, throughout. To quantitate symptoms subjects were asked to score (from 0, none, to 6, severe) six neurogenic (autonomic) symptoms - heart pounding, shaky/tremulousness and nervous/anxious (adrenergic) and sweaty, hungry and tingling (cholinergic) - and six neuroglycopenic symptoms - difficulty thinking/confused, tired/drowsy, weak, warm, faint and dizzy (15). After completion of the glucose clamps/PET studies on Day 1 interprandial plasma glucose concentrations were held at $\sim 55 \text{ mg/dL}$ (3.0 mmol/L) with variable intravenous insulin infusions until they were increased to 90 mg/dl [5.0 mmol/L] at the start of the clamps on the morning of Day 2.

Neuroendocrine and Metabolic Analytical Methods

Plasma glucose concentrations were measured with a glucose oxidase method (YSI Glucose Analyzer 2, Yellow Springs Instruments, Yellow springs, OH). Plasma epinephrine and norepinephrine concentrations were measured with a single isotope derivative (radioenzymatic) method (16) and plasma insulin (17), C-peptide (17), glucagon (18), pancreatic polypeptide (19), cortisol (20) and growth hormone (21) were measured with radioimmunoassays. Serum nonesterified fatty acid (22) and blood lactate (23) concentrations were measured with enzymatic techniques.

Relevant systemic variables during euglycemia on Days 1 and 2 and during hypoglycemia on Days 1 and 2 were contrasted with a t-test for paired data. P values less than 0.05 were considered to indicate significant differences.

Positron Emission Tomography (PET) and Magnetic Resonance (MR) Imaging

PET studies were performed with a Siemens/CTI (Knoxville, TN) ECAT EXACT HR 47 tomograph located in the Neurology-Neurosurgery Intensive Care Unit PET Research Facility (24). Subjects were positioned in the tomograph such that the entire brainstem was included within the 15 cm axial field of view. As a result, the vertex of the brain was not included within the study area. An individual transmission scan was obtained for each subject and used for subsequent attenuation correction of emission scan data. Regional cerebral blood flow (rCBF) was measured with a 40 sec emission scan after bolus intravenous injection of 50 mCi of [^{15}O]water ($1 \text{ Ci} = 37 \text{ GBq}$) using an adaptation of the Kety autoradiographic method (25-27). PET scans were acquired in the two-dimensional mode (interslice septa extended).

PET images were reconstructed using filtered back projection and measured attenuation. Each subject's attenuation correction was co-registered to each emission scan prior to the final reconstruction in order to eliminate spatial variation in attenuation from each individual's difference images. Reconstructed images were smoothed with a 3-D Gaussian filter to a resolution of 10 mm full-width at half-maximum. Next, each subject's images were co-registered to each other (28), and the mean of all of that subject's images was co-registered to a standard mean blood flow image in Talairach atlas space (29). All individual images were normalized using mean whole-brain counts. The 4 euglycemic and the 4 hypoglycemic images for each subject were combined into single state images for each day to increase statistical precision (30). Images of regional CBF differences between euglycemia and hypoglycemia on Day 1 and on Day 2 were created by image subtraction. For the group data these two subtraction images, each representing the regions of brain activation during acute hypoglycemia on each day, were examined for differences with SPM99 (31) using a fixed effects model with multiple comparisons correction for the entire volume. T values were computed at each voxel, and clusters of at least 90 voxels (1 resel) with uncorrected $P < 0.005$ were identified. The statistical significance of these clusters was computed and corrected for the number of possible clusters of their size and magnitude within the brain volume (32,33). This analysis determines areas where differences in CBF occur without any pre-specification of regions of interest. Location of regions of significant change is expressed in x, y, z, stereotactic coordinates in mm with positive values representing right, anterior, and superior respectively (29).

Each subject also underwent structural magnetic resonance (MR) imaging of the brain with a 1.5 T system (Magnetom Sonata, Siemens, Erlangen, Germany). A three dimensional magnetization-prepared rapid gradient echo (MPRAGE) sequence (1900/1100/3.9 repetition time/ inversion time/echo time (ms); flip angle = 15°) was acquired in a sagittally oriented plane (160 mm thick, 128 partitions, 256 mm field of view) and reconstructed into a 256×256 matrix ($1 \times 1 \times 1.25$ mm pixels).

Results

Plasma Insulin C-peptide and Glucose and Glucose Infusion Rates (Table 1)

Plasma insulin concentrations were raised substantially and plasma glucose targets were met during the euglycemic and hypoglycemic clamps on Days 1 and 2 (Table 1). Glucose infusion rates required to maintain both the euglycemic and the hypoglycemic clamps were lower, following interval hypoglycemia, on Day 2 (Table 1). Plasma C-peptide concentrations were suppressed during hypoglycemic clamps on both Days (Table 1).

Symptomatic Neuroendocrine and Metabolic Responses to Hypoglycemia (Table 1)

Symptom scores and plasma epinephrine, glucagon, pancreatic polypeptide and cortisol concentrations during hypoglycemia were reduced, following interval hypoglycemia, on Day 2, as were the required glucose infusion rates and blood lactate concentrations. Serum nonesterified fatty acid concentrations were suppressed under these hyperinsulinemic conditions.

Regional Cerebral Blood Flow (Figure 1)

The regional CBF patterns during euglycemia on Day 2, following interval hypoglycemia, were not different from those on Day 1 (data not shown). The only brain region that showed a significantly greater increase in CBF during hypoglycemia on Day 2 compared to Day 1 was the thalamus (corrected $P = 0.004$). The size of the significant Day 2 cluster was 207 voxels. The region of CBF change was centered in the left pulvinar ($x = -14$, $y = -30$, $z = 7$) and included the dorsal medial and paraventricular nuclei of the thalamus bilaterally (Figure 1) (34).

Discussion

These data again document that recent antecedent hypoglycemia - here ~12-14 hours of interval interprandial hypoglycemia - produces in healthy humans (10) a model of hypoglycemia-associated autonomic failure (HAAF) in diabetes (1-3) including the key feature of HAAF, an attenuated sympathoadrenal response to subsequent hypoglycemia. Compared with the responses on Day 1, the adrenomedullary plasma epinephrine response and the largely sympathetic neural symptomatic response (4) (among other responses) to hypoglycemia were reduced on Day 2, following interval hypoglycemia. Thus, the phenomenon we sought to explain mechanistically, HAAF in diabetes, was produced experimentally in these nondiabetic individuals.

We have used the technique of measuring changes in regional CBF with positron emission tomography (PET) to identify regions of increased synaptic activity during hypoglycemia (13). This approach requires that the physiological coupling between increases in neuronal activity and increases in regional CBF remains intact under these conditions. We have previously shown that this coupling is preserved with arterial hypoglycemia to 2.3 mmol/L (41 mg/dL) (35). We measured regional CBF on two consecutive days with interval hypoglycemia. Repeat PET CBF studies show no significant differences within the same scanning session (36). Furthermore, [¹⁸F]deoxyglucose PET studies of metabolism performed 1 to 18 days apart show no changes in thalamic uptake normalized for whole brain counts as was done here (37,38). In the present study the regional CBF patterns during euglycemia on Day 2 were not different from these on Day 1. Therefore, the observed difference in the regional CBF response to hypoglycemia is unlikely to be an order effect. Areas of increased CBF primarily reflect the increased metabolic activity of synaptic fields, not the spike firing rate of neuronal cell bodies (39,40). Thus, the definitive finding of this study was a significantly greater increase in synaptic activity in the dorsal midline thalamus during recurrent hypoglycemia with attenuated counterregulatory responses as compared to initial hypoglycemia with robust counterregulatory responses. The center of this region is virtually identical ($x = -14$, $y = -30$, $z = 7$) to the region of increase during initial hypoglycemia ($x = -11$, $y = -23$, $z = 6$) that we identified in our previous study as part of a brain network that mediates autonomic responses to various stimuli and includes the dorsal medial and paraventricular nuclei of the thalamus bilaterally (14). The finding of greater synaptic activity associated with attenuated counterregulatory responses indicates that the dorsal midline thalamus plays an active inhibitory role in reducing the sympathoadrenal and symptomatic responses to hypoglycemia when previous hypoglycemia has occurred, the key feature of HAAF in diabetes.

Sympathoadrenal (and glucagon) responses to systemic hypoglycemia are directly stimulated by reduced local hypothalamic glucose concentrations (41-44). These responses are reduced by both lesions of the ventromedial hypothalamus and by maintenance of high extracellular hypothalamic glucose concentrations (41,42). They can be mimicked by selective hypothalamic cellular glucopenia with systemic euglycemia (43). In chronically systemically hypoglycemic rats, the epinephrine responses to selective hypothalamic cellular glucopenia with systemic euglycemia are attenuated. This observation is consistent with inhibition of the normal hypothalamic response to hypoglycemia in response to antecedent hypoglycemia (44).

Given the role of the hypothalamus as the central integrator of the sympathoadrenal response to hypoglycemia (41-44), the novel finding reported here extends the regulation of the sympathoadrenal response to include the dorsal midline thalamus. To our knowledge there is no precedent for a role of the dorsal midline thalamus in the regulation of the sympathoadrenal response to hypoglycemia. However, that region of the thalamus includes the paraventricular nucleus of the thalamus (PVNT) and there is evidence that activation of the PVNT mediates

habituation of the pituitary-adrenocortical response to recurrent restraint stress in rats (45). Therefore, given the present finding, it is reasonable to suggest that increased PVNT activation might mediate habituation of the sympathoadrenal response to recurrent hypoglycemia in humans, the key feature of HAAF in diabetes. Indeed, given the neuroanatomical connections of the dorsal midline thalamus and their physiological functions (46-54) we could postulate a cerebral network - including the medial prefrontal cortex, orbito-medial prefrontal cortex, hippocampus, amygdala, periaqueductal grey and thalamus - regulating the hypothalamic response to recurrent hypoglycemia. Clearly, however, the documentation and definition of such a cerebral network awaits further study.

This construct of the pathophysiology of HAAF is consistent with the findings of Cranston et al. (55). Using [¹⁸F]deoxyglucose and positron emission tomography, they found that deoxyglucose uptake decreased in the subthalamic region of the brain during hypoglycemia in patients with T1DM and hypoglycemia unawareness whereas it was little changed in patients with hypoglycemia awareness. Since that subthalamic region is centered in the hypothalamus, it may well have been inhibited by the increased thalamic activity documented in the present study.

To unequivocally establish the causal nature of thalamic activation in HAAF will require demonstration that direct inhibition or ablation of dorsal medial thalamic nuclei prevents attenuation of counterregulatory responses to recurrent hypoglycemia. Surgically implanted electrodes in the thalamus, currently used to treat intractable tremor, provide a means to further investigate this mechanism and may in the future offer a novel approach to treatment of HAAF (56).

Acknowledgements

This study was supported, in part, by National Institutes of Health (NIH) grants R37 DK27085, MO1 RR00036, P60 DK20579 and by Washington University in St. Louis and the University of North Carolina. A.M. Arbelaez was supported, in part, by NIH grant K12 DK63683.

The authors acknowledge the assistance of the staff of the Washington University General Clinical Research Center in the performance of this study; the technical assistance of Krishan Jethi, Michael Orasco, Gene Wade Sherrow, Michael Morris, Zina Lubovich, Sharon Travis and Sharon O'Neil; and the assistance of Janet Dedek in the preparation of this manuscript. We would also like to thank Lori McGee-Minnich, Lennis Lich, the Washington University Medical School Cyclotron Staff and the East Building Magnetic Resonance Imaging Facility staff for their assistance.

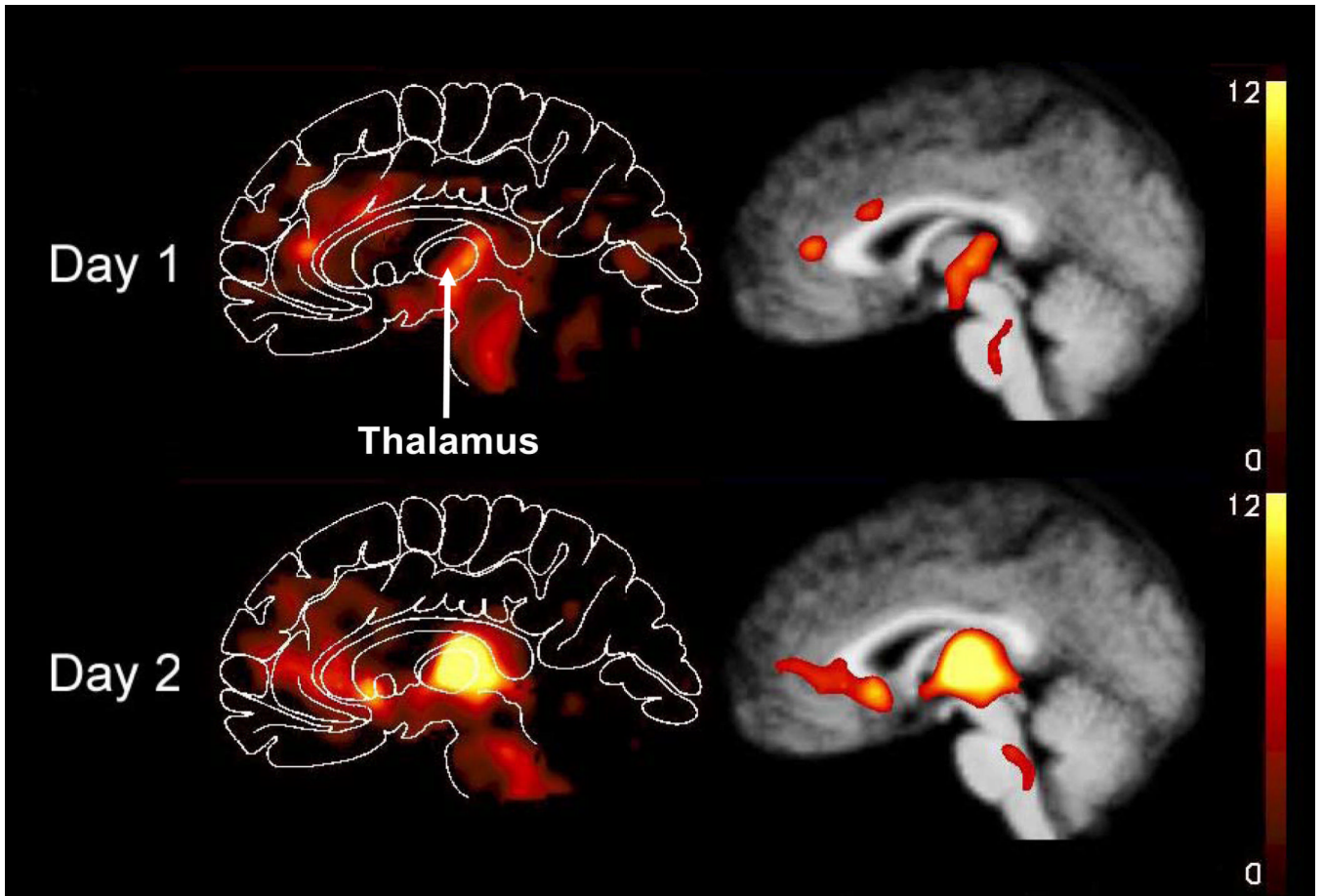
References

1. Cryer PE. Diverse causes of hypoglycemia-associated autonomic failure in diabetes. *N Engl J Med* 2004;350:2272–2279. [PubMed: 15163777]
2. Dagogo-Jack SE, Craft S, Cryer PE. Hypoglycemia-associated autonomic failure in insulin-dependent diabetes mellitus. *J Clin Invest* 1993;91:819–828. [PubMed: 8450063]
3. Segel SA, Paramore DS, Cryer PE. Hypoglycemia-associated autonomic failure in advanced type 2 diabetes. *Diabetes* 2002;51:724–733. [PubMed: 11872673]
4. DeRosa MA, Cryer PE. Hypoglycemia and the sympathoadrenal system: Neurogenic symptoms are largely the result of sympathetic neural, rather than adrenomedullary, activation. *Am J Physiol Endocrinol Metab* 2004;287:E32–E41. [PubMed: 14970007]
5. Gold AE, MacLeod KM, Frier BM. Frequency of severe hypoglycemia in patients with type 1 diabetes with impaired awareness of hypoglycemia. *Diabetes Care* 1994;17:697–703. [PubMed: 7924780]
6. White NH, Skor DA, Cryer PE, Levandoski LA, Bier DM, Santiago JV. Identification of type 1 diabetic patients at increased risk for hypoglycemia during intensive therapy. *N Engl J Med* 1983;308:485–491. [PubMed: 6337335]

7. Bolli GB, De Feo P, De Cosmo S, Perriello G, Ventura MM, Benedetti MM, Santeusano F, Gerich JE, Brunetti P. A reliable and reproducible test for adequate glucose counterregulation in type 1 diabetes. *Diabetes* 1984;33:732–737. [PubMed: 6378698]
8. Ertl AC, Davis SN. Evidence for a vicious cycle of exercise and hypoglycemia in type 1 diabetes mellitus. *Diabetes Metab Res Rev* 2004;20:124–130. [PubMed: 15037987]
9. Banarar S, Cryer PE. Sleep-related hypoglycemia-associated autonomic failure in type 1 diabetes: Reduced awakening from sleep during hypoglycemia. *Diabetes* 2003;52:1195–1203. [PubMed: 12716752]
10. Segel SA, Fanelli CG, Dence CS, Markham J, Videen TO, Paramore DS, Powers WJ, Cryer PE. Blood-to-brain glucose transport, cerebral glucose metabolism and cerebral blood flow are not increased following hypoglycemia. *Diabetes* 2001;50:1911–1917. [PubMed: 11473055]
11. Cryer PE. Mechanisms of hypoglycemia-associated autonomic failure and its component syndromes in diabetes. *Diabetes* 2005;54:3592–3601. [PubMed: 16306382]
12. Cryer PE. Mechanisms of sympathoadrenal failure and hypoglycemia in diabetes. *J Clin Invest* 2006;116:1470–1473. [PubMed: 16741570]
13. Raichle ME. Behind the scenes of functional brain imaging: a historical and physiological perspective. *Proc Natl Acad Sci USA* 1998;95:765–772. [PubMed: 9448239]
14. Teves D, Videen TO, Cryer PE, Powers WJ. Activation of human medial prefrontal cortex during autonomic responses to hypoglycemia. *Proc Natl Acad Sci USA* 2004;101:6217–6221. [PubMed: 15026569]
15. Towler DA, Havlin CE, Craft S, Cryer PE. Mechanism of awareness of hypoglycemia: Perception of neurogenic (predominantly cholinergic) rather than neuroglycopenic symptoms. *Diabetes* 1993;42:1791–1798. [PubMed: 8243825]
16. Shah SD, Clutter WE, Cryer PE. External and internal standards in the single isotope derivative (radioenzymatic) measurement of plasma norepinephrine and epinephrine. *J Lab Clin Med* 1985;106:624–629. [PubMed: 4067376]
17. Kuzuya H, Blix PM, Horwitz DL, Steiner DF, Rubenstein AH. Determination of free and total insulin and C-peptide in insulin-treated diabetics. *Diabetes* 1977;26:22–29. [PubMed: 830562]
18. Ensink, J. Immunoassays for glucagon. In: Lefebvre, P., editor. *Handbook of Experimental Pharmacology*. 66. Springer Verlag; New York: 1983. p. 203-221.
19. Gingerich RL, Lacy PE, Chance RE, Johnson MG. Regional pancreatic concentration and in vitro secretion of canine pancreatic polypeptide, insulin and glucagon. *Diabetes* 1978;27:96–101. [PubMed: 203506]
20. Farmer RW, Pierce CE. Plasma cortisol determination: Radioimmunoassay and competitive protein binding compared. *Clin Chem* 1974;20:411–414. [PubMed: 4856379]
21. Schlach D, Parker M. A sensitive double antibody radioimmunoassay for growth hormone in plasma. *Nature* 1964;703:1141–1142.
22. Hosaka K, Kikuchi T, Mitsuhide N, Kawaguchi A. A new colorimetric method for determination of free fatty acids with acyl-CoA synthase and acyl-CoA oxidase. *J Biochem (Tokyo)* 1981;89:1799–1803. [PubMed: 7287653]
23. Lowry O, Passoneau J, Hasselberger F, Schultz D. Effect of ischemia on known substrates and co-factors of the glycolytic pathway of the brain. *J Biol Chem* 1964;239:18–30. [PubMed: 14114842]
24. Wienhard K, Dahlbom M, Ericksson L, Michel C, Bruckbauer T, Pietrzyk U, Heiss WD. The ECAT EXACT HR: performance of a new high resolution positron scanner. *J Comput Assist Tomogr* 1994;18:110–118. [PubMed: 8282858]
25. Herscovitch P, Markham J, Raichle MR. Brain blood flow measured with intravenous H₂(15)O. I. Theory and error analysis. *J Nucl Med* 1983;24:782–789. [PubMed: 6604139]
26. Raichle ME, Martin WR, Herscovitch P, Mintun MA, Markham J. Brain blood flow measured with intravenous H₂(15)O. II. Implementation and validation. *J Nucl Med* 1983;24:790–798. [PubMed: 6604140]
27. Videen TO, Perlmutter JS, Herscovitch P, Raichle ME. Brain blood volume, flow, and oxygen utilization measured with ¹⁵O radiotracers and positron emission tomography: revised metabolic computations. *J Cereb Blood Flow Metab* 1987;7:513–516. [PubMed: 3497165]

28. Woods RP, Cherry SR, Mazziotta JC. Rapid automated algorithm for aligning and reslicing PET images. *J Comput Assist Tomogr* 1992;16:620–633. [PubMed: 1629424]
29. Talairach, J.; Tournoux, P. Thieme; New York: 1988. Co-Planar Stereotaxic Atlas of the Human Brain.
30. Ingvar M, Eriksson L, Greitz T, Stone-Elander S, Dahlbom M, Rosengvist G, af Trampe P, von Euler C. Methodological aspects of brain activation studies: cerebral blood flow determined with [¹⁵O] butanol and positron emission tomography. *J Cereb Blood Flow Metab* 1994;14:628–638. [PubMed: 8014210]
31. Statistical Parametric Mapping. www.fil.ion.ucl.ac.uk/spm
32. Friston KJ, Holmes AP, Worsley KJ, Poline JP, Frith CD, Frackowiak RSJ. Statistical parametric maps in functional imaging: A general linear approach. *Hum Brain Mapp* 1995;2:189–210.
33. Worsley KJ, Marrett S, Neelin P, Vandal AC, Friston KJ, Evans AC. A unified statistical approach for determining significant signals in images of cerebral activation. *Hum Brain Mapp* 1996;4:58–73.
34. Rieck RW, Ansari MS, Whetsell WO Jr, Deutch AY, Kessler RM. Distribution of dopamine D2-like receptors in the human thalamus: autoradiographic and PET studies. *Neuropsychopharmacology* 2004;29:362–372. [PubMed: 14627996]
35. Powers WJ, Hirsch IB, Cryer P. Effect of stepped hypoglycemia on regional cerebral blood flow response to physiological brain activation. *Am J Physiol* 1996;270:H554–H559. [PubMed: 8779830]
36. Matthew E, Andreason P, Carson RE, Herscovitch P, Pettigrew K, Cohen R, King C, Johanson CE, Paul SM. Reproducibility of resting cerebral blood flow measurements with H₂(¹⁵O) positron emission tomography in humans. *J Cereb Blood Flow Metab* 1993;13:748–754. [PubMed: 8360281]
37. Bartlett EJ, Brodie JD, Wolf AP, Christman DR, Laska E, Meissner M. Reproducibility of cerebral glucose metabolic measurements in resting human subjects. *J Cereb Blood Flow Metab* 1988;8:502–512. [PubMed: 3260593]
38. Stapleton JM, Morgan MJ, Liu X, Yung BCK, Phillips RL, Wong DF, Shaya EK, Dannals RF, London ED. Cerebral glucose utilization is reduced in second test session. *J Cereb Blood Flow Metab* 1997;17:704–712. [PubMed: 9236727]
39. Mathiesen C, Caesar K, Akgören N, Lauritzen M. Modification of activity-dependent increases of cerebral blood flow by excitatory synaptic activity and spikes in rat cerebellar cortex. *J Physiol* 1998;512:555–566. [PubMed: 9763643]
40. Schwartz WJ, Smith CB, Davidsen L, Savaki H, Sokoloff L, Mata M, Fink DJ, Gainer H. Metabolic mapping of functional activity in the hypothalamo-neurohypophysial system of the rat. *Science* 1979;205:723–725. [PubMed: 462184]
41. Borg WP, During MJ, Sherwin RS, Borg MA, Brines ML, Shulman GI. Ventromedial hypothalamic lesions in rats suppress counterregulatory responses to hypoglycemia. *J Clin Invest* 1994;93:1677–1682. [PubMed: 8163668]
42. Borg MA, Sherwin RS, Borg WP, Tamborlane WV, Shulman GI. Local ventromedial hypothalamus glucose perfusion blocks counterregulation during systemic hypoglycemia in awake rats. *J Clin Invest* 1997;99:361–365. [PubMed: 9006005]
43. Borg WP, Sherwin RS, During MJ, Borg MA, Shulman GI. Local ventromedial hypothalamus glucopenia triggers counterregulatory hormone release. *Diabetes* 1995;44:180–184. [PubMed: 7859938]
44. Borg MA, Borg WP, Tamborlane WV, Brines ML, Shulman GI, Sherwin RS. Chronic hypoglycemia and diabetes impair counterregulation induced by localized 2-deoxyglucose perfusion of the ventromedial hypothalamus in rats. *Diabetes* 1999;48:584–587. [PubMed: 10078560]
45. Bhatnagar S, Huber R, Nowak N, Trotter P. Lesions of the posterior paraventricular thalamus block habituation of hypothalamic-pituitary-adrenal responses to repeated restraint. *J Neuroendocrinol* 2002;14:403–410. [PubMed: 12000546]
46. Bhatnagar S, Viau V, Chu A, Soriano L, Meijer OC, Dallman MF. A cholecystokinin-mediated pathway to the paraventricular thalamus is recruited in chronically stressed rats and regulates hypothalamic-pituitary-adrenal function. *J Neurosci* 2000;20:5564–5573. [PubMed: 10884340]
47. Otake K, Kin K, Nakamura Y. Fos expression in afferents to the rat midline thalamus following immobilization stress. *Neurosci Res* 2002;43:269–282. [PubMed: 12103445]

48. Ongür D, Price JL. The organization of networks within the orbital and medial prefrontal cortex of rats, monkeys and humans. *Cereb Cortex* 2000;10:206–219. [PubMed: 10731217]
49. Herman JP, Figueiredo H, Mueller NK, Ulrich-Lai Y, Ostrander MM, Choi DC, Cullinan WE. Central mechanisms of stress integration: hierarchical circuitry controlling hypothalamo-pituitary-adrenocortical responsiveness. *Front Neuroendocrinol* 2003;24:151–180. [PubMed: 14596810]
50. Moga MM, Weis RP, Moore RY. Efferent projections of the paraventricular thalamic nucleus in the rat. *J Comp Neurol* 1995;359:221–238. [PubMed: 7499526]
51. Spencer SJ, Fox JC, Day TA. Thalamic paraventricular nucleus lesions facilitate central amygdala neuronal responses to acute psychological stress. *Brain Res* 2004;997:234–237. [PubMed: 14706875]
52. Huang H, Ghosh P, van den Pol AN. Prefrontal cortex-projecting glutamatergic thalamic paraventricular nucleus-excited by hypocretin: a feedforward circuit that may enhance cognitive arousal. *J Neurophysiol* 2006;95:1656–1668. [PubMed: 16492946]
53. Rempel-Clower NL, Barbas H. Topographic organization of connections between the hypothalamus and the prefrontal cortex in the rhesus monkey. *J Comp Neurol* 1998;398:393–419. [PubMed: 9714151]
54. Figueiredo HF, Bruestle A, Bodie B, Dolgas CM, Herman JP. The medial prefrontal cortex differentially regulates stress-induced c-fos expression in the forebrain depending on type of stressor. *Eur J Neurosci* 2003;18:2357–2364. [PubMed: 14622198]
55. Cranston I, Reed LJ, Marsden PK, Amiel SA. Changes in regional brain ¹⁸F-fluorodeoxyglucose uptake at hypoglycemia in type 1 diabetic men associated with hypoglycemia unawareness and counter-regulatory failure. *Diabetes* 2001;50:2329–2366. [PubMed: 11574416]
56. Perlmutter JS, Mink JW. Deep brain stimulation. *Annu Rev Neurosci* 2006;29:229–257. [PubMed: 16776585]



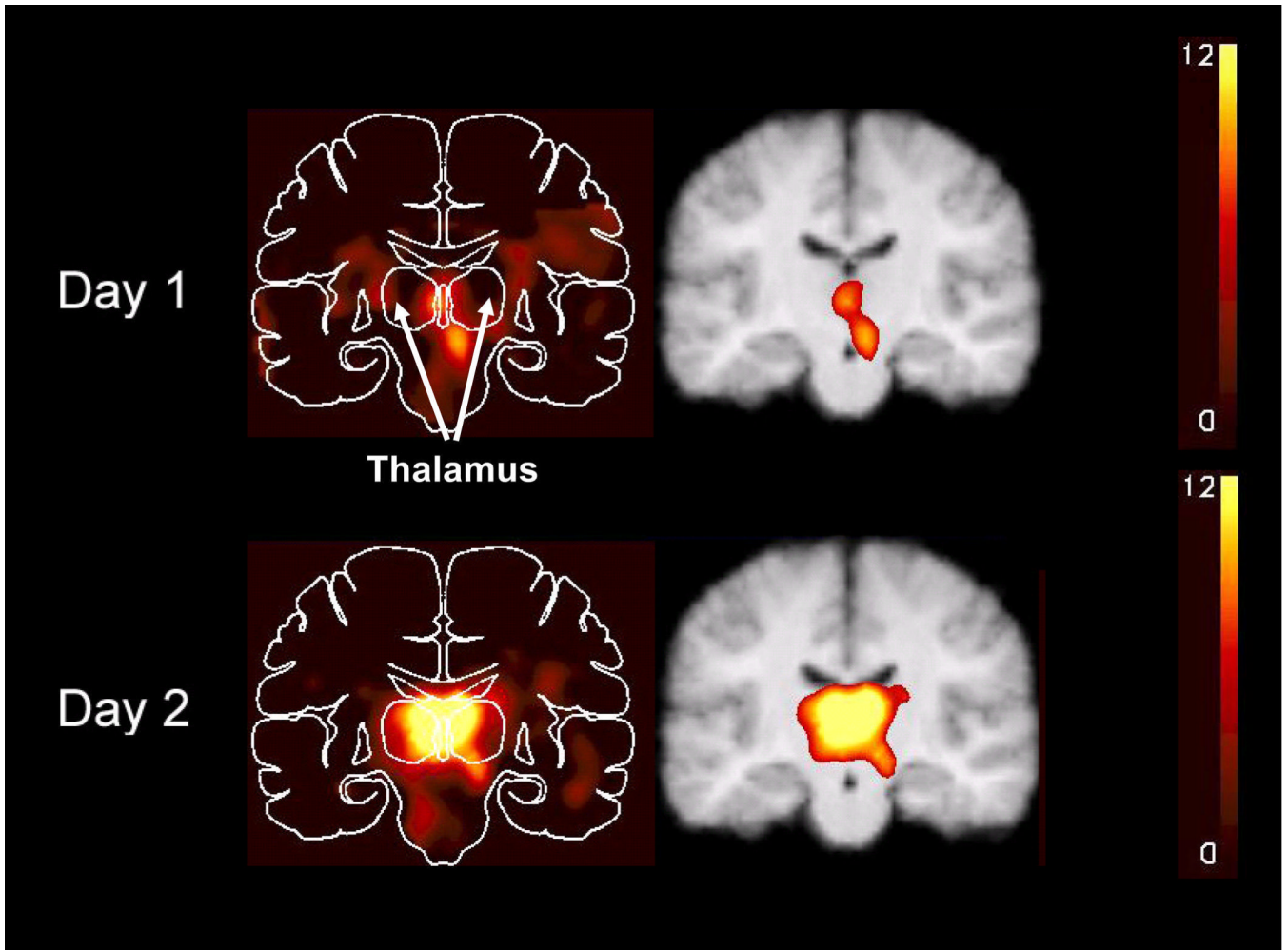


Figure 1.

Regional cerebral blood flow changes during hypoglycemia illustrating greater synaptic activity in bilateral dorsal midline thalamus on Day 2, following ~24 hours of interval interprandial hypoglycemia, compared with Day 1. These are combined subtraction images from all PET scans from all nine subjects superimposed on the combined MR image. The color scales show changes relative to mean global blood flow. A maximum of 12% is used for all scales. However, the maximum change for Day 2 was 18% compared with 10% on Day 1. A. Mid-sagittal slices. B. Coronal slices at the level of the paraventricular nuclei ($y = -19$) with the left of the brain on the left (33).

Table 1

Mean (\pm SE) neuroendocrine, metabolic and symptom values during the second hour (at the times of the PET scans) of clamped euglycemia and hypoglycemia on Day 1 and, after interval interprandial hypoglycemia (\sim 55 mg/dL [3.0 mmol/L]), on Day 2. The statistical contrasts shown are between Day 1 and Day 2

	---Euglycemia---		--Hypoglycemia--	
	Day 1	Day 2	Day 1	Day 2
Insulin (μ U/mL)	103 \pm 5	93 \pm 4	97 \pm 6	87 \pm 6
Glucose (mg/dL)	90 \pm 1	91 \pm 1	55 \pm 1	54 \pm 1
Glucose Infusion Rate ($\text{mg}\cdot\text{kg}^{-1}\cdot\text{min}^{-1}$)	8.7 \pm 0.9	4.4 \pm 0.6 ^a	6.5 \pm 0.6	5.2 \pm 0.8 ^e
C-peptide (ng/mL)	1.0 \pm 0.1	0.7 \pm 0.1 ^c	0.4 \pm 0.0	0.4 \pm 0.0
Symptom Score	4.8 \pm 1.2	3.5 \pm 0.4	10.1 \pm 1.6	5.8 \pm 0.8 ^e
Epinephrine (pg/mL)	44 \pm 18	45 \pm 12	365 \pm 96	149 \pm 27 ^b
Norepinephrine (pg/mL)	207 \pm 26	239 \pm 12	300 \pm 32	266 \pm 16
Glucagon (pg/mL)	77 \pm 7	67 \pm 6	107 \pm 9	80 \pm 7 ^a
Pancreatic Polypeptide (pg/mL)	67 \pm 12	65 \pm 9	553 \pm 71	100 \pm 29 ^e
Cortisol (μ g/dL)	11.8 \pm 1.4	12.0 \pm 1.8	18.0 \pm 2.8	13.1 \pm 1.5 ^d
Growth Hormone (ng/mL)	0.2 \pm 0.1	1.1 \pm 0.3	17.5 \pm 1.0	15.9 \pm 2.7
Lactate (mmol/L)	1.21 \pm 0.13	0.80 \pm 0.11 ^b	31 \pm 0.13	0.79 \pm 0.09 ^c
Nonesterified Fatty Acids (μ mol/L)	161 \pm 25	237 \pm 79	167 \pm 28	245 \pm 62

To convert insulin to pmol/L multiply by 6.0, glucose to mmol/L multiply by 0.05551, glucose infusion rate to $\mu\text{mol}\cdot\text{kg}^{-1}\cdot\text{min}^{-1}$ multiply by 5.551, c-peptide to nmol/L multiply by 0.331, epinephrine to pmol/L multiply by 5.458, norepinephrine to nmol/L multiply by 0.005911, glucagon to pmol/L multiply by 0.239, pancreatic polypeptide to pmol/L multiply by 0.239, cortisol to nmol/L multiply by 27.59, and growth hormone to pmol/L multiply by 44.15.

^aP<0.0001

^bP<0.001

^cP<0.01

^dP<0.02

^eP<0.05